A Dual-Channel Microwave Radiometer for Measurement of Precipitable Water Vapor and Liquid

FRED O. GUIRAUD, MEMBER, IEEE, JOE HOWARD, AND DAVID C. HOGG, FELLOW, IEEE

Abstract—**The design and performance of a two-channel ground-based microwave radiometer (20.6 and 31.6 GHz) for measurement of total integrated water vapor and cloud liquid in a vertical column are discussed. Unique features of this instrument are a single antenna producing equal beamwidth for the two frequencies, and incorporation of two stable reference loads in a three-way Dicke switching sequence. The latter allows an automatic gain control (AGC) to be applied in a minicomputer. Linear statistical inversion is used to retrieve the precipitable water vapor and liquid quantities which are provided in real time. The instrument has been in reliable operation, continuously and unattended, at the National Weather Service Forecast Office, Denver, CO, for a six-month period. The radiometrically derived precipitable water vapor compares favorably with that obtained from radiosondes.**

I. INTRODUCTION

MICROWAVE radiometers provide essentially continuous remote sensing of atmospheric variables such as temperature, water vapor, and liquid. Because of the characteristics of absorption by the gases and liquid, wavelengths of about 1 cm and less are suitable for the measurement of temperature, vapor, and cloud liquid, whereas wavelengths of several centimeters are needed to measure heavy rain. Thus the word "essentially" in the first sentence means that observations of temperature and vapor are meaningful except during conditions of medium and heavy rainfall when millimeter-wave radiometers saturate (i.e., the brightness temperature approaches ambient). But experience [1] and analysis [2] show that reliable observations can be made in the presence of any cloud that is not producing rain. Neither dry snow nor clouds formed of ice particles affect the radiometers. Thus unlike infrared radiometric methods, microwave remote sensing results in accurate observation of atmospheric variables for a large percentage of the time.

We discuss here the design and implementation of a radiometric system that operates continuously and unattended at the frequencies 20.6 and 31.6 GHz (wavelengths 1.45 and 0.95 cm). The objective is to provide reliable measurements of total precipitable water vapor and path-average cloud liquid (in the zenith direction) for research in weather forecasting. This dual-channel radiometer constitutes a subsystem of a remote-sensing profiler system which is being developed to profile temperature and wind continuously. The profiler system, in turn, forms an element of PROFS[1].

The dual-channel radiometer has other special applications. For example, the variable phase shift that limits the resolution of large interferometers [3] and arrays used in microwave radio astronomy is directly related to the path-average water vapor between the elements of the interferometer and the radio source. An independent and accurate measure of the vapor allows correction of the phase shift. Since the vapor and liquid phases of water are measured simultaneously and independently, application in weather modification is also feasible.

The role played by continuous measurement of precipitable water vapor in weather forecasting is by no means clear. Examples of data given here show that during the 12-h interval between launches of radiosondes, large amounts of vapor can pass over a location unobserved by the sondes. However, it is believed that as such data become available, the significance of the small-scale variations in vapor (and in cloud liquid) will become useful in forecasting precipitation.

A. The Radiometric System

1) General Description: The prototype radiometric system consists of two radiometers, one at a frequency of 20.6 GHz, near the water vapor absorption line at 22.2 GHz, and the second at 31.6 GHz in the transmission window above the line. The 20.6-GHz brightness temperature responds primarily to vapor and the 31.6-GHz to liquid (see Fig. 1(a)). The two radiometers are coupled to a single offset parabolic reflector antenna using an orthomode coupler. This antenna, along with the radiometers, is located inside the small building shown in Fig. 2. Energy from the zenith is reflected in a horizontal beam, toward the antenna, by a 45° high-quality flat reflector. Two sheets of 2-mil Mylar separated with an air gap of approximately 2 in form a low-loss window to pass the microwave energy into the building; an aluminum cowling shields the Mylar window from all but the strongest wind-blown rain (see also sketch in Fig. 4). The flat reflector can be rotated about a horizontal axis, allowing measurements to

Manuscript received March 29, 1979; revised July 12, 1979.

The authors are with the Environmental Radiometry, Wave Propagation Laboratory, NOAA/Environmental Research Laboratories, Boulder, CO 80303.

[1]PROFS is a Prototype Regional Observing and Forecasting Service that encompasses observation, forecasting, and dissemination of regional weather information.

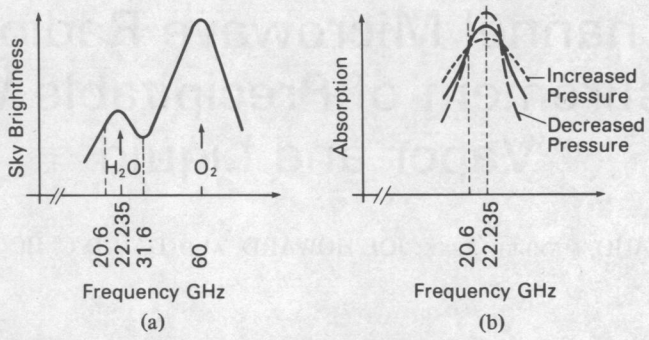

Fig. 1. Location of radiometric frequencies for the precipitable water vapor–liquid radiometers and curves illustrating the effect of pressure broadening of the water-vapor absorption line.

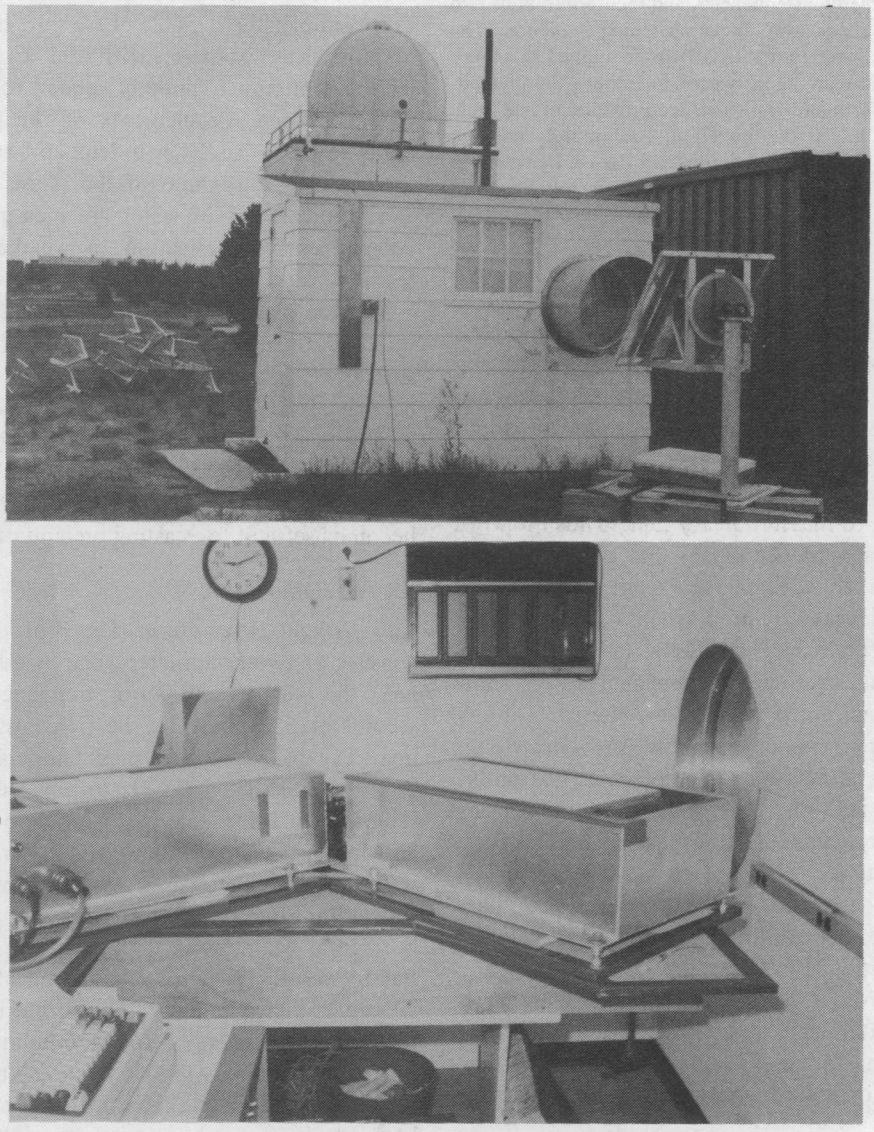

Fig. 2. Exterior–interior views of the radiometric installation.

be made at different elevation angles. The outputs from the radiometers along with the temperatures of critical waveguide components, necessary in the reduction of the measurements, are passed to a mini-computer for real-time linear statistical solutions for the total precipitable water vapor (V) and cloud liquid (L). The data from the radiometers are stored on the minicomputer's floppy diskette. The V-L data are also displayed on strip chart, a digital panel display, and teletype-terminal printout.

The choice of the lower frequency at 20.6 GHz, slightly below the peak of the 22-GHz vapor line, can be explained by reference to Fig. 1(b) which shows an exaggeration of the

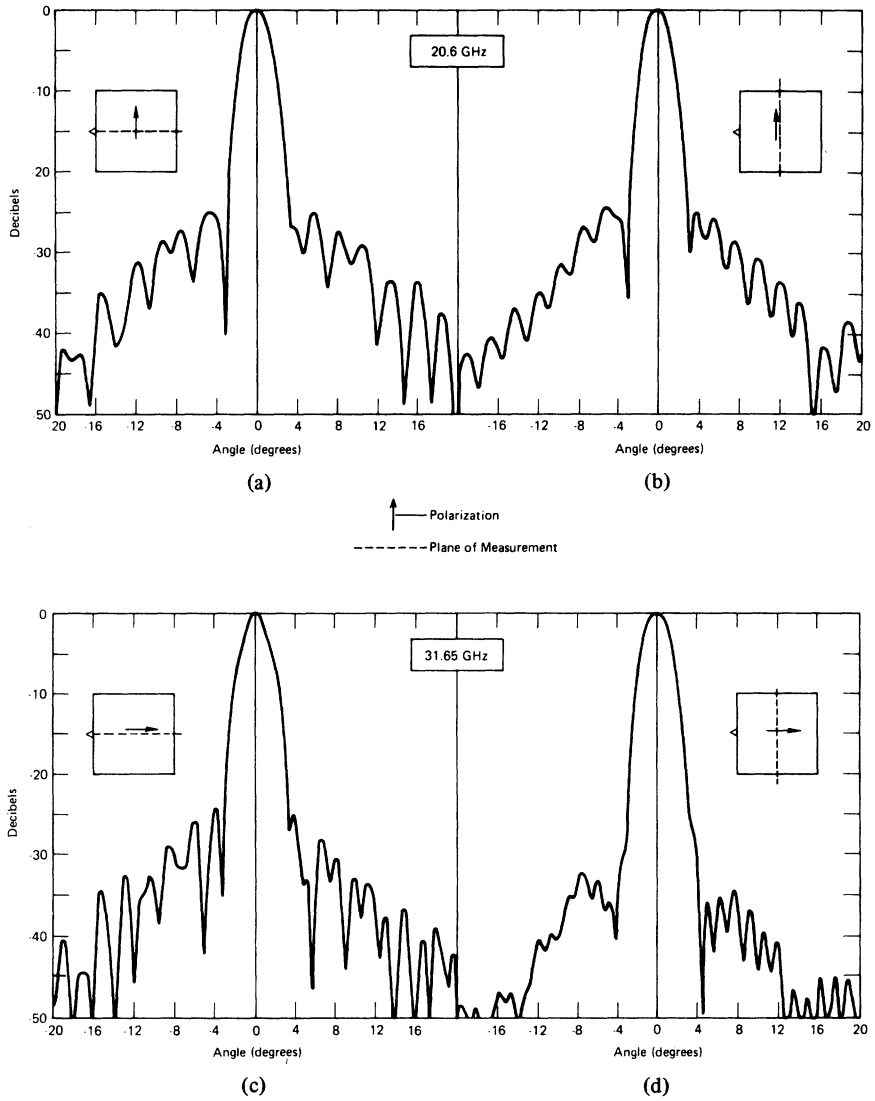

Fig. 3. Radiation patterns of the equal beam antenna at 20.6 and 31.6 GHz.

effect of pressure on broadening of the line. As pressure increases, the absorption at the center of the line decreases, and conversely, it increases in the wings. However, as illustrated, absorption is nearly invariant with pressure at the 20.6-GHz point [4]. Since the amount of water vapor in the atmosphere is highly variable with height, the small pressure dependence obtained by operation at 20.6 GHz is highly desirable. The 31.6-GHz frequency was selected since it is in the window between the water vapor and oxygen lines, and is in a protected space-research band.

The design of this instrument is directed toward an all-weather capability, and proper antenna performance is very important in achieving this goal. Especially when liquid-bearing clouds are present, and drift through the antenna beams, it is desirable that the two radiometers sense the same volume; this requires equal antenna beamwidths for the two frequencies. With proper selection of reflector and feed horn, two frequencies can be supported simultaneously in a single antenna and nearly equal beamwidths can be produced over a rather large bandwidth, in this case from 21 to 31 GHz, about 40 percent [5]. The behavior of the feed horn is such that the reflector is under-illuminated at the higher frequency, while the lower frequency, supported in the same feed horn, illuminates more of the reflector; this results in different effective apertures for the two frequencies and thus in equal beams.

Beam patterns for the antenna are shown in Fig. 3. The 51 X 51 cm reflector was machined from aluminum to an rms surface tolerance of approximately 0.05 mm. The focal length of the reflector is 40 cm and is fed by a hybrid-mode horn whose aperture is 5 cm. The surface of the flat reflector, located outside the building, has been shimmed and supported to obtain a flatness of about 0.08 mm rms. The surface is painted with a flat white paint to aid in the sheeting of rain droplets and to speed up the purging of liquid from the surface. Liquid water on this reflector surface does not cause as large an error in measurement as it would on the Mylar window into the building. But the indicated precipitable water vapor can be increased by as much as 3 mm, as shown by wetting the reflector's surface artificially on a clear stable day.

2) RF Operation: The basic circuits of the two radiometers are identical and are shown in the block diagram, Fig. 4. Table I lists the specifications for the radiometers. They follow a traditional design, but in this case, operated with a three-way

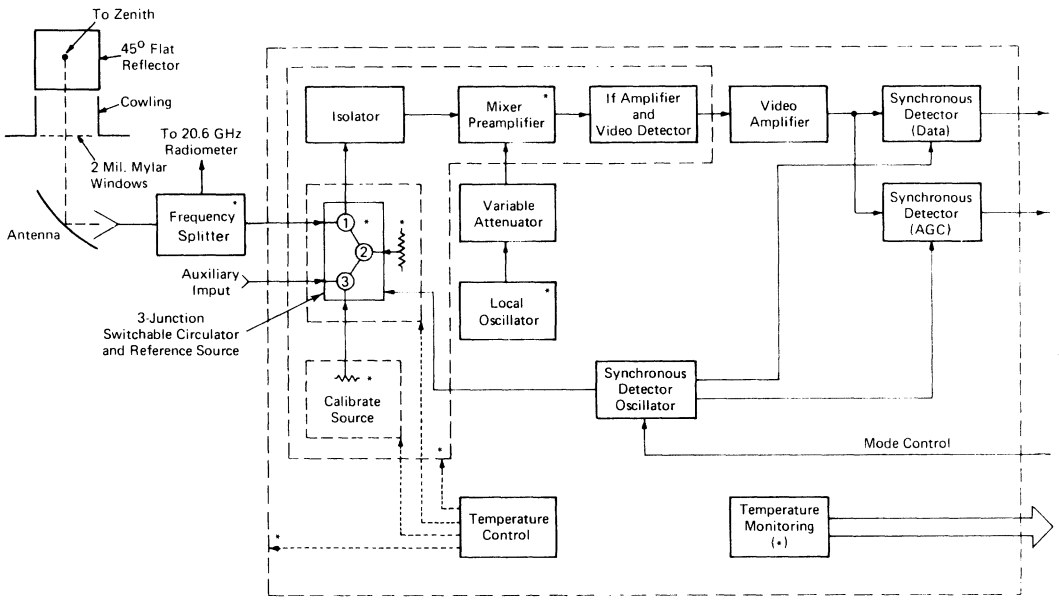

Fig. 4. Plan view in block-diagram form for the radiometer.

TABLE I
NOAA LIQUID-VAPOR RADIOMETERS (SPECIFICATIONS)

Channel	Vapor	Liquid
Center Frequency	20.6 GHz	31.6 GHz
RF Bandwidth	∿ 500 MHz	∿ 500 MHz
Receiver Noise Temperature (not including antenna)	675 K	875 K
Sensitivity (1 sec RC)	0.10 K	0.12 K
Antenna Beamwidth (3 dB)	2.4°	2.2°
Post-Detection Integration Time	1.0 sec	1.0 sec

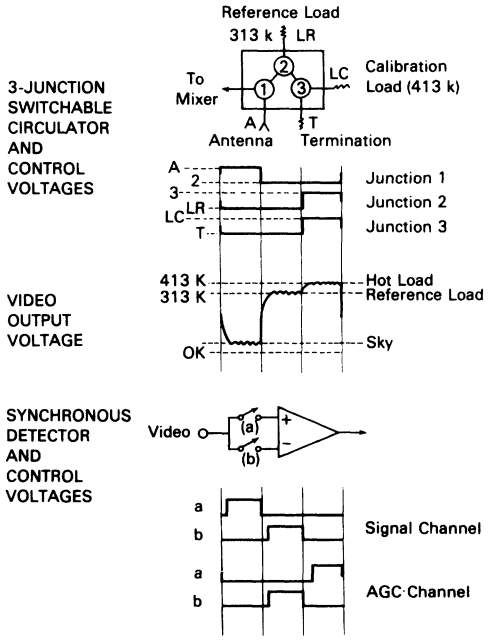

Fig. 5. Waveforms of the control voltages of the radiometer.

rather than a two-way switch. For good operational performance, high-quality Schottky-barrier mixers followed by wide-band pre- and post-IF amplifiers are used. Heated waveguide terminations are used for reference sources rather than cryogenically cooled sources, which present problems operationally.

The principle of operation can be understood by following the switching sequences in Fig. 5. The three-junction latching circulator samples the noise power sequentially from the antenna, a temperature-controlled reference source (45°C), and a calibration source (145°C). After being amplified and detected, the signal from the video amplifier appears as a three-step staircase. Synchronous detection for the signal is accomplished by gating an operational amplifier when switched to the antenna and the reference source; the resultant output is integrated before being sent to the computer. However, with only this mode of operation, very high stability on the gain of all amplifiers in the system would be required. For this reason the calibrate source (145°C) is added to the switching sequence. Then, by adding a second synchronous detector, and gating this detector to the calibration and reference sources, its output becomes a continuous monitor of any gain fluctuation that occurs in the system. This latter output provides a voltage for an automatic gain control (AGC); the AGC is actually effected in the computer.

The logic for the switchable circulator and the gating for the synchronous detectors is PROM-controlled. Not only is it necessary to maintain the correct phase relationship between the circulator and synchronous detectors, but a 0.1-ms time delay must also be allowed in order that the signal settle following a change in the state of the circulator. Two other programs are also stored in the PROM to provide control sequences to the synchronous detectors for calibration. Because the timing programs for the controls are in PROM, adjustments can easily be made if modifications are desired.

Although the gain variations in the system are monitored by the AGC signal as discussed above, these variations are initially minimized by temperature control. The radiometers, already located in a heated and air conditioned room, are further

stabilized by temperature-controlled heating of a styrofoam-lined enclosure. Further temperature stabilization is achieved by mounting the mixer preamplifier, IF amplifier, video detector, and local oscillator on an aluminum plate, which is also temperature-stabilized at approximately 40°C, which is 5°C above the temperature of the enclosure.

Finally, the circulator and the reference-source termination are stabilized near 45°C and the calibration source near 145°C, all being appropriately insulated. Lengths of 1-in gold-plated thin-wall stainless-steel waveguide reduce heat transfer through the waveguides. The reference and calibrate sources drift less than 0.02°C rms for weekly periods. The temperature-control circuitry in each case consists of a thermistor in a bridge network as input to a voltage comparator. AC voltage-to-heating resistors is controlled by the comparator in a simple off-on mode through a solid-state relay. In addition to control of the temperatures, linearized thermistors are located in each area of control for monitoring of temperature.

3) Data Transfer: A 16-channel 10-bit A-D converter is used to sample the signal and AGC voltages, the temperatures of the reference and calibrate sources, and the temperature of the antenna feed horn, including the waveguide runs outside the temperature-controlled enclosure. Several other temperatures are monitored that are not needed directly in the reduction of the measurements but are useful in evaluating the performance of the radiometers. The A-D converter samples at a rate of 10 samples per second; these are averaged for 10 s before being reduced to precipitable water by the minicomputer. The 10-s V-L values are converted to analog voltages, which are displayed on panel meters and strip charts. The unreduced 10-s data are further averaged over 2-min periods before being recorded on the computer's floppy diskette. Since the component temperatures change slowly, they are averaged over 20-min periods, and also are recorded on the floppy diskette.

Periodically, the current 2-min averaged data are reduced to precipitable water vapor and integrated liquid. These quantities are tabulated and displayed in a simple symbol plot. An example of the display, in 30-min intervals, is given in Fig. 6; this is available on the minicomputer's terminal and on a remote terminal, via a leased telephone line, at the Denver Weather Service Forecast Office (WSFO).

All of the averaging periods mentioned above are software selectable and are set when the acquisition program is initiated. The periods chosen are based primarily on the storage capacity of the floppy diskette. At the above rates the radiometers can be operated for approximately 9 days before the diskette is filled.

B. Calibration

To provide best accuracy in the calibrations discussed here, derivations from Planck's radiation law rather than the Rayleigh-Jeans approximation are used to describe the microwave brightness temperature of a partially absorbing body of absorption, "a":

$$\frac{(1 - e^{-a})}{e^{hf/kT_m} - 1} = \frac{1}{e^{hf/kT_b} - 1} \tag{1}$$

DAY	TIME MST	VAP CM	LIQ CM	0 1 2 3 4 123456789 123456789 123456789 123456789 V-CM, L-MM
10/	0 0	0.68	0.01	+L V + + + +
10/	0:30	0.68	0.02	L V
10/	1: 0	0.66	0.02	L V
10/	1 30	0.66	0.01	L V
10/	2: 0	0.64	0.00	L V
10/	2:30	0.63	0.00	L V
10/	3: 0	0.64	0.00	L V + + + +
10/	3:30	0.66	0.00	L V
10/	4: 0	0.61	0.00	L V
10/	4:30	0.56	0.00	L V
10/	5: 0	0.56	0.00	L V
10/	5:30	0.56	0.00	L V
10/	6: 0	0.53	0.00	L V + + + +
10/	6:30	0.54	0.00	L V
10/	7: 0	0.55	0.00	L V
10/	7:30	0.54	0.00	L V
10/	8: 0	0.56	0.00	L V
10/	8:30	0.55	0.00	L V
10/	9: 0	0.54	-0.01	L V + + + +
10/	9:30	0.55	0.00	L V
10/10:	0	0.56	0.00	L V
10/10:	30	0.57	0.00	L V
10/11:	0	0.54	0.00	L V
10/11:	30	0.55	0.00	L V
10/12:	0	0.53	0.00	L V + + + +
10/12:	30	0.53	0.00	L V
10/13:	0	0.52	0.00	L V
10/13:	30	0.54	0.00	L V
10/14:	0	0.54	0.00	L V
10/14:	30	0.57	0.00	L V
10/15:	0	0.57	0.00	L V + + + +
10/15:	30	0.59	0.00	L V
10/16:	0	0.63	0.00	L V
10/16:	30	0.67	0.00	L V
10/17:	0	0.67	0.00	L V
10/17:	30	0.75	0.00	L V
10/18:	0	0.71	0.00	L V + + + +
10/18:	30	0.73	0.00	L V
10/19:	0	0.72	0.00	L V
10/19:	30	0.72	0.00	L V
10/20:	0	0.71	0.00	L V
10/20:	30	0.71	0.00	L V
10/21:	0	0.67	0.00	L V + + + +
10/21:	30	0.67	0.00	L V
10/22:	0	0.71	-0.01	L V
10/22:	30	0.70	-0.01	L V
10/23:	0	0.71	-0.01	L V
10/23:	30	0.71	-0.01	L V

Fig. 6. Teletype record at the WSFO for precipitable water vapor (V) and integrated cloud liquid (L) (January 10, 1979); clouds bearing a small amount of liquid are overhead from 00:30 to 01:30.

where

T_b	mean brightness temperature (K),
h	Planck's constant (J · s),
f	microwave frequency (Hz),
k	Boltzmann's constant (J · K^{-1}),
T_m	mean temperature of the body (K),
kT_bB	microwave power,
B	bandwidth.

Within a temperature-controlled environment a calibration at one point in a network of lossy waveguides may be transferred to another point by applying an appropriate factor for the intervening loss. In the present system the factor transfers from the hot calibration and reference sources to the Dicke switch (see Junction 1 of Fig. 5). The losses through the external waveguides to the antenna input must also be accounted for; since these are outside the temperature-controlled area, corrections for self-emission at the temperature of the waveguide (which is measured) must also be made.

Zenith sky emission can be found independently and used to determine the above transfer factors. This independent procedure [6] requires a set of radiometric measurements at different elevation angles (i.e., a "tipping" curve, or elevation scan), a measurement of emission from a sheet of good microwave absorber, and knowledge of the mean temperature of the atmosphere. The zenith brightness temperature determined in this way is insensitive to the mean temperature of the

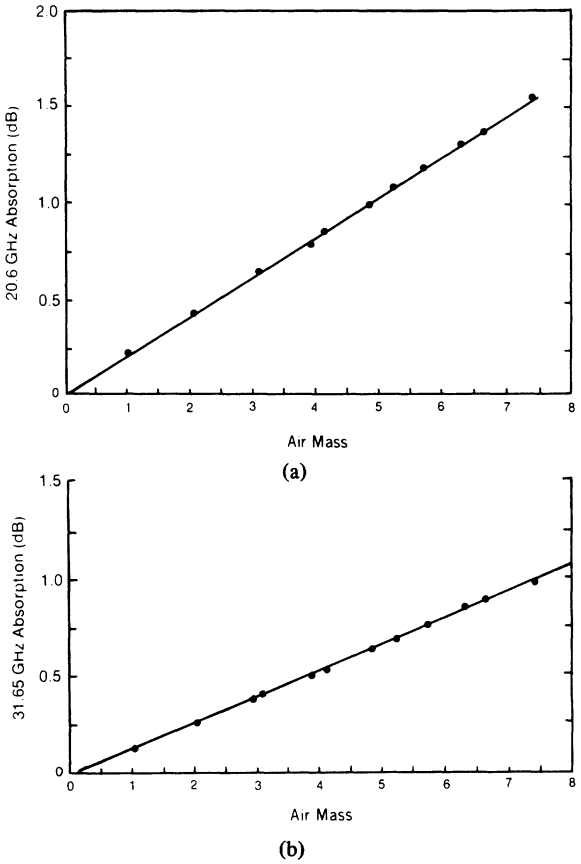

Fig. 7. Typical measurement of absorption on a clear day obtained from a scan in elevation.

atmosphere T_m, and a value of 270 K is adequate, but in any case, for calibration, T_m can be obtained from radiosondes on clear days. An example of a tipping curve used to establish the zenith brightness temperature is shown in Fig. 7. The atmospheric absorption must pass through zero absorption at zero air mass. If it does not, the original estimate of zenith brightness temperature used in deriving the absorption (see (1)) is wrong; the correct value is found by iterating until the appropriate sky brightness that forces the absorption through zero at zero air mass. Cosmic background (2.9 K attenuated by the atmospheric absorption) is included in the procedure.

Our calibration transfer factors were determined from an average of 30 tipping curves. Fig. 8(a) and (b) show, as scatter plots, the sky brightnesses measured directly on the calibrated zenith-looking radiometer compared with those obtained from tipping curves.

The short-term (hours) stability of the overall instrument can be seen in Fig. 9, which shows the precipitable water vapor measured on an extremely dry day when the atmosphere was very stable. During the period between 8 and 10 h, the rms variation in precipitable water vapor is only 70 μm. This is the same variation we achieve when directing the antenna beam at a microwave absorber; thus we believe 70 μm to be the short-term stability of the instrument.

C. Retrieval Algorithms

Statistical retrieval algorithms [1] are used for the determination of the precipitable water vapor and liquid. A relationship between V or L and the independent measurements

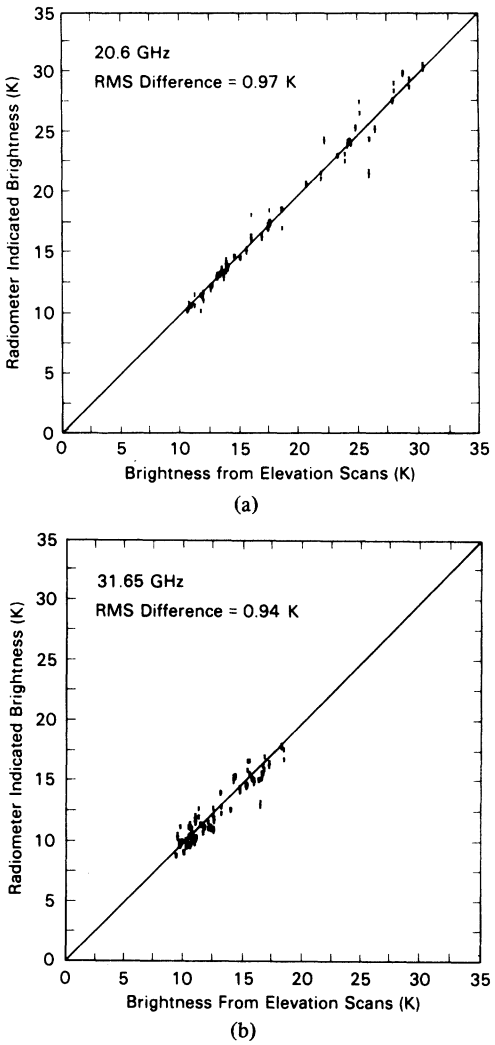

Fig. 8. Clear-sky calibration summary for 20.6 and 31.6 GHz from June 1978 through August 1978.

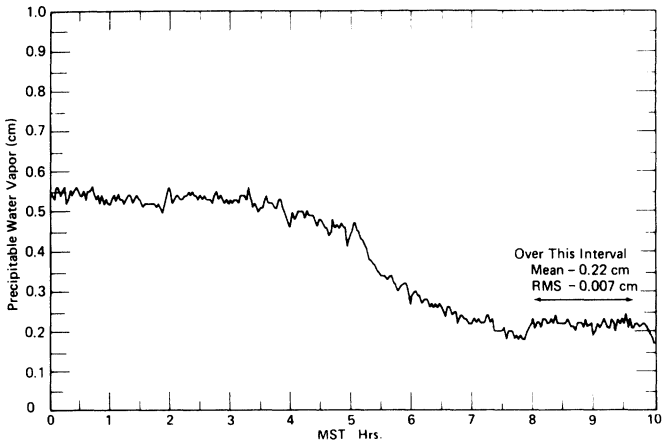

Fig. 9. Radiometrically measured total-precipitable water vapor at Denver, CO, WSFO December 13, 1978; the measurements are 2-min averages on a clear, very dry day.

of brightness temperatures from the two radiometric channels is established in this way. The coefficients are derived from *a priori* statistics (i.e., a historical sample) of a suitable set of radiosonde profiles. The precipitable water vapor and the coefficients are readily obtained using this set of radiosonde

profiles. L is more difficult, since radiosondes do not measure liquid, and little information on integrated cloud liquid is available from other sources. Therefore, in developing *a priori* statistics for the L coefficients, a model cloud is inserted into every radiosonde profile whose relative humidity exceeds 95 percent [1]. The cloud-liquid density is varied as a function of the thickness of the 95-percent layer. A random error of 1 K is included in the theoretical brightness temperatures to simulate instrumental error. Coefficients have been derived from 6 years of radiosonde profiles measured at Denver, CO. V and L are taken to be linear with brightness temperature (see (2)).

We have found from our measurements that the absorption coefficients for water vapor used previously in our algorithms [7], resulted in derived vapor that was too low by brightness of approximately 7 percent. As a first-order[2] correction for this effect, we simply multiplied the coefficients in the retrieval algorithms by 1.07.

For Denver, CO., the relationships are

$$V = -0.19 + 0.118\,T_b(20.6) - 0.0560\,T_b(31.6)$$

$$L = -0.018 - 0.00114\,T_b(20.6) + 0.0284\,T_b(31.6) \qquad (2)$$

where V and L are in centimeters and T_b is in kelvin.

We have had no independent measurement of the integrated liquid and, therefore, no standard for comparison. However, a method using combined satellite-signal attenuation and radiometric techniques has recently been instrumented [8] to provide such an independent measure.

D. Behavior in Operation at a WSFO

Since, at this writing, the dual-channel system has been in operation for more than 6 months at a WSFO radiosonde launch site, considerable experience on accuracy and reliability has been gained.

A typical analog plot of total precipitable water vapor above the Denver, CO, WSFO, taken over a 2-week period, is shown in Fig. 10. The solid curve is radiometrically measured and the triangles are total precipitable water vapor from integrated radiosonde data, which are obtained at 12-h intervals. The agreement is quite good. Of the differences that do exist on individual readings, we do not know how much is due to the radiometric system and how much is error stemming from the radiosonde measurement. It is clear, however, that during certain 12-h intervals (e.g., August 8, P.M. to August 9, A.M.), considerable amounts of vapor pass overhead unobserved by the sondes.

Further verification of performance is obtained by plotting precipitable water vapor amounts by the radiometer and the radiosonde directly against one another as in Fig. 11. In this 6-month sample, the rms difference between the two is 1.7 mm, some part of this being attributable to each measuring device. Although establishment of the error in operational-radiosonde measurements is difficult, estimates by experienced operators and researchers, for typical midrange humidity and temperature, place $\overline{(V_S - V_A)^2}$ at $(1.5\text{ mm})^2$, where V_S is the

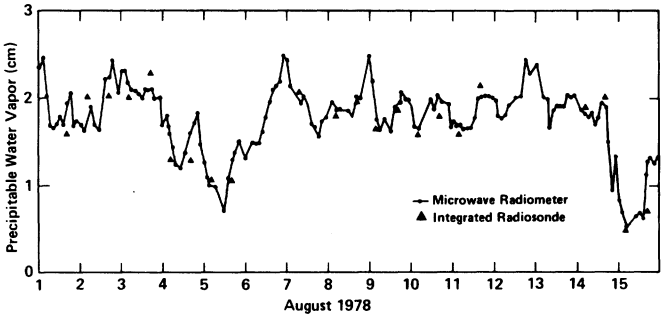

Fig. 10. Measurements of precipitable water vapor at Denver, CO, for a 15-day period in August 1978.

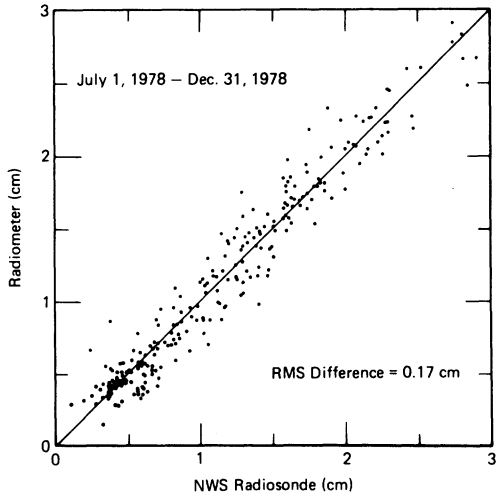

Fig. 11. Scatter plot for a 6-month measurement period at Denver, CO, comparing total precipitable water vapor from radiometers with radiosonde measurements.

sonde-measured precipitable water vapor and V_A is the actual value.[3] Thus assuming no correlation between radiosonde and radiometric errors, one obtains

$$\overline{(V_R - V_A)^2} = 1.7^2 - 1.5^2 = 0.65$$

or 0.8 mm for the rms error of the radiometric measurement. However, all that can really be said reliably is that the radiometric values are about the same or better than those of the radiosonde.

It should be emphasized that all data for the 6 months, regardless of weather conditions, are plotted in Fig. 11 for those times when total precipitable water vapor from the radiosonde was available. This remark points to the fact that many cases involving clouds are included. The error in precipitable water vapor that is associated with a nonprecipitating cloud of given integrated liquid can be calculated [2]; computations for the 20.6/31.6-GHz system are shown in Fig. 12. The upper abscissa gives the 31-GHz attenuation corresponding to the integrated cloud liquid on the lower abscissa. The particular set of curves in Fig. 12, calculated assuming 0.5 K rms noise in the radiometric system, is carried to cloud liquid of about 10 mm, although most nonprecipitating clouds we

[2]We also measure a quadratic component in absorption as a function of precipitable water, especially at 31.6 GHz, [10], but that effect is not yet included in the retrieval algorithm.

[3]The radiosonde values for total precipitable water vapor at Denver are obtained from the Bureau of Reclaimation (Denver) computer which simply integrates the raw data from the radiosondes.

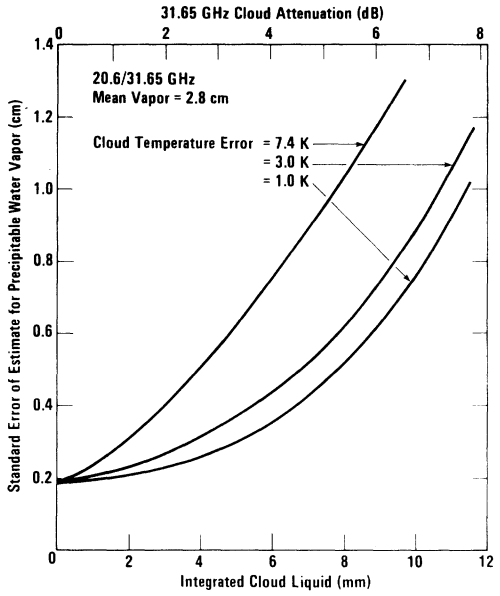

Fig. 12. Predicted error in radiometrically derived precipitable water vapor in the presence of increasing quantities of cloud liquid.

observe at Denver contain less than 2 mm. The three curves of the set correspond to various errors in knowledge of the temperature of the liquid in the cloud; the most pessimistic, 7.4 K, is the estimate of climatological error in cloud-liquid temperature. In that case, a cloud producing a line integral 3 mm of liquid (31-GHz attenuation about 2 dB) results in an error of 0.4 cm in the precipitable water vapor, which is about 15 percent of the mean (2.8 cm) assumed in Fig. 12.

Algorithms for retrieving precipitable water vapor during rain have not yet been developed; therefore, if rain occurs at the time of printout to the WSFO (Fig. 6), no data are transmitted. Nevertheless, the radiometers operate satisfactorily (remain below saturation) up to attenuations of at least 6 dB at 30 GHz. This magnitude of attenuation would be produced by a rain of rate 10 mm/h originating at a height 3 km above the site [9]. In the operational mode, if the 30-GHz brightness temperature exceeds 100 K (about 2 dB of attenuation), the data are not forwarded to the WSFO.

Rain also produces a systematic error in measurement by way of wetting of the flat reflector shown in Fig. 2(a). This effect has been measured by spraying the reflector with water on a clear day. It is found that apparent increases in precipitable water vapor of 0.2 to 0.3 cm can be produced. An air curtain above the reflector to blow aside rain and wet snow[4] before it reaches the reflector is under investigation. In an operational system, such an air curtain would be activated by a device that independently monitors the presence of precipitation.

[4]Dry snow on the reflector has little effect.

II. Conclusion

Construction and evaluation of the performance of a dual-channel microwave radiometer has shown that continuous and unattended measurement of precipitable water vapor and cloud liquid is operationally viable. Long-term (months) errors in the vapor retrieved from the radiometric measurement are shown to be of the same order as those of the radiosonde. Short-term (hours) stability of the retrieved precipitable water vapor is within 0.01 cm. Continuous measurement of the precipitating clouds is shown to be achieved with good accuracy; however, accurate measurement in the presence of rain has yet to be demonstrated.

Acknowledgment

The authors thank E. B. Burton for hospitality at the National Weather Service Forecast Office, Denver, CO, and A. B. Duncan of the Wave Propagation Laboratory, for help with the measurements.

References

[1] M. T. Decker, E. R. Westwater, and F. O. Guiraud, "Experimental evaluation of ground-based microwave radiometric sensing of atmospheric temperature and water vapor profiles," *J. Appl. Meteorol.*, vol. 17, no. 12, Dec. 1978.

[2] E. R. Westwater, "The accuracy of water vapor and cloud liquid determination by dual-frequency ground-based microwave radiometry," *Radio Sci.*, vol. 13, no. 4, pp. 677-685, 1978.

[3] R. Hinder and M. Ryle, "Atmospheric limitation to the angular resolution of aperture synthesis radio telescopes," *Mon. Notic. Roy. Astron. Soc.*, vol. 154, pp. 229-253, 1971.

[4] E. R. Westwater, "An analysis of the correction of ray errors due to atmospheric refraction by microwave radiometric techniques," ESSA Tech. Rep., IER 30-ITSA 30, 1967.

[5] D. C. Hogg, F. O. Guiraud, J. Howard, A. C. Newell, D. P. Kremer, and A. G. Repjar, "An antenna for dual-wavelength radiometry at 21 and 32 GHz," *IEEE Trans. Antennas Propagat.*, vol. AP-27, Nov. 1979.

[6] F. O. Guiraud and D. C. Hogg, "A noise-temperature measurement of spillover in the horn-reflector antenna," *IEEE Trans. Antennas Propagat.*, vol. AP-27, Mar. 1979.

[7] E. R. Westwater, "Microwave emission from clouds," NOAA Tech. Rep., ERL-219-WPL-18, 1972.

[8] J. B. Snider, "Measurement of cloud liquid content using the 28 GHz COMSTAR beacon," presented at the USNC/URSI Symp., Seattle, WA, June 18-22, 1979.

[9] D. C. Hogg and T. S. Chu, "The role of rain in satellite communication," *Proc. IEEE*, vol. 63, pp. 1308-1331, Sept. 1975.

[10] D. C. Hogg and F. O. Guiraud, "Microwave measurements of the absolute values of absorption by water vapour in the atmosphere," *Nature*, vol. 279, May 31, 1979.